Case Studies in Construction Materials 12 (2020) e00342

Contents lists available at ScienceDirect

Case Studies in Construction Materials

journal homepage: www.elsevier.com/locate/cscm

Case study

Effect of geocomposite reinforcement on the performance of thin asphalt pavements: Accelerated pavement testing and laboratory analysis

Lorenzo Paolo Ingrassia*, Amedeo Virgili, Francesco Canestrari

Università Politecnica delle Marche, Via Brecce Bianche, 60131, Ancona, Italy

ARTICLE INFO

Article history:
Received 16 October 2019
Received in revised form 20 December 2019
Accepted 7 February 2020

Keywords:
Thin asphalt pavements
APT
FastFWD
Geocomposites

ABSTRACT

The objective of this study is to assess the effect of geocomposite reinforcement on fatigue cracking, reflective cracking and permanent deformation accumulation of thin asphalt pavements. For this purpose, a full-scale trial section was constructed with different interfaces: unreinforced (reference) and reinforced with three types of geocomposites, formed by the combination of a bituminous membrane with a fabric or grid. The experimental program included accelerated pavement testing (APT) carried out by means of Fast Falling Weight Deflectometer (FastFWD) and laboratory tests (three point bending tests) on samples taken from the trial section. After APT, significant permanent deflections were observed, likely due to the plastic yielding of the unbound layers. Nevertheless, all the geocomposites improved the permanent deformation resistance as compared to the unreinforced pavement by reducing the vertical strain at the top of the subgrade. Moreover, the geocomposites increased the energy necessary for the crack propagation by three to eight times with respect to the unreinforced pavement. Overall, these findings indicate that the use of geocomposites can extend the service life of thin asphalt pavements in terms of both cracking and permanent deformation accumulation.

1. Introduction

Reinforcement systems are often placed within the layers in asphalt pavements for maintenance and rehabilitation purposes, with the aim of preventing or delaying the development of cracks. These systems can considerably increase the maintenance intervals of asphalt pavements, resulting in a cost-effective and long-lasting pavement rehabilitation method. Moreover, they can be considered sustainable solutions, as they also allow to reduce the thickness of the old layers to be milled and of the new layers to be constructed, with consequent environmental benefits such as lower exploitation of new raw materials, reduced production, transportation, lay-down and compaction of asphalt and less materials to be disposed of. Among the various reinforcement systems available on the market, a noteworthy solution is represented by geocomposites that combine the tensile properties of a reinforcing material with the stress-relieving and waterproofing effects of a bituminous membrane.

Several studies [1–9] have demonstrated that the use of geogrids, geosynthetics and geocomposites in asphalt pavements can effectively extend the fatigue life, enhance the resistance to reflective cracking and improve the rutting resistance. On the

* Corresponding author.
E-mail addresses: l.p.ingrassia@pm.univpm.it (L.P. Ingrassia), a.virgili@univpm.it (A. Virgili), f.canestrari@univpm.it (F. Canestrari).

https://doi.org/10.1016/j.cscm.2020.e00342

other hand, the presence of such type of reinforcements at the interface determines a significant reduction of the interlayer shear resistance [2,10–12].

In recent years, accelerated pavement testing (APT) has become a major tool to assess the long-term in-situ pavement performance, because it can simulate, in a relatively short period of time, the damage accumulation throughout the service life of the pavement due to vehicular traffic [13].

Within this framework, the objective of this study was to investigate the effect of geocomposites (formed by the combination of a bituminous membrane with a fabric or grid) on the performance of thin asphalt pavements in terms of fatigue cracking, reflective cracking and permanent deformation accumulation. A full-scale trial section, characterized by different types of interfaces (reinforced with geocomposites and unreinforced), was constructed and APT was performed using Fast Falling Weight Deflectometer (FastFWD). Moreover, the investigation was completed by laboratory tests (three point bending tests) on samples taken from the trial section. The laboratory results were also compared with those obtained in a previous experimental investigation carried out on laboratory-compacted slabs with the same geocomposites at the interface, in order to evaluate the reliability of laboratory tests for predicting the field behaviour of geocomposites.

2. Experimental program

2.1. Trial section description

A full-scale trial section was constructed in July 2018 in Pegognaga (Italy) on an existing pavement inside an industrial area. The trial section included four test fields characterized by different interfaces, as follows:

- reinforced with geocomposite 1 (coded as R1);
- reinforced with geocomposite 2 (coded as R2);
- reinforced with geocomposite 3 (coded as R3);
- reference unreinforced, with a tack-coat interface (coded as UN).

Each test field, 8 m long and 3 m wide, was divided into two sections in order to study the performance in terms of fatigue cracking and reflective cracking, referred to as FC and RC, respectively.

The existing pavement was composed of 9 cm of asphalt concrete (AC) and 30 cm of thick granular subbase course. For the construction of the trial section, 6 cm of asphalt concrete were milled. In each RC section, the milled surface was then cut with a square 20 cm mesh in order to simulate a pre-existing crack network. Afterwards, the reinforced test fields were prepared by placing the geocomposites (R1, R2 and R3) directly over the milled surface, while a conventional tack-coat bituminous emulsion was applied on the milled surface of the unreinforced section (UN). To promote the adhesion with the milled surface, some passages with the steel roller were carried out after the application of the geocomposites. Finally, the new AC course layer (5 cm thick) was laid-down at about 150 °C and compacted at 5 % target air void content [14].

2.2. Materials

For the new AC course, a dense graded asphalt mixture was used, characterized by maximum aggregate dimension size of 12.5 mm and bitumen content (50/70 unmodified bitumen) of 4.4 % by aggregate weight.

Three geocomposites (R1, R2 and R3) were used as reinforcement. R1 and R2 had a thickness of 2.5 mm and were manufactured with a styrene-butadiene-styrene (SBS) polymer modified bitumen. The lower surface presented an auto-adhesive film, whereas the upper surface was a polypropylene non-woven fabric. Based on the product datasheet, the upper side was characterized by a melting temperature of about 130–140 °C. The main difference between R1 and R2 was the type of geosynthetic within the geomembrane. In fact, R1 was reinforced with a stabilized continuous fiberglass fabric, characterized by a nominal tensile strength of 40 kN/m (in both longitudinal and transverse direction), whereas R2 was reinforced with a non-woven polyester fabric and multidirectional fiberglass, characterized by a nominal tensile strength of 35 kN/m (in both directions). In addition, R2 was characterized by a greater tensile elongation at failure with respect to R1 (30 % in both directions for R2 vs. 6 % in both directions for R1). R3 was composed of an elastomeric (SBS-modified) bituminous membrane combined with a fiberglass grid having a mesh size of 12.5 × 12.5 mm^2. The upper surface of the geocomposite was coated with a fine sand whereas the lower surface presented an auto-thermo-adhesive SBS-modified bituminous film. R3 had a thickness of 2.5 mm (as R1 and R2) and was characterized by a tensile strength of 40 kN/m and a tensile elongation at failure lower than 4 % in both the longitudinal and transverse direction.

2.3. Testing program and procedures

The testing program was divided into two parts. In the first part, the in-situ investigation of the full-scale trial fields was carried out by APT tests, performed by means of a FastFWD device, developed by Dynatest in 2015 in order to speed up the experimental procedures through a loading rate from 5 to 7.5 times faster than the traditional FWD device [15]. The FastFWD was configured with a 30 cm diameter loading plate and nine geophones positioned at 0, 20, 30, 45, 60, 90, 120, 150 and 180

cm from the center of the loading plate. For each test field, two APT sessions were carried out both on FC section and RC section, as summarized in Table 1.

During the two APT sessions, the FastFWD device was removed at regular intervals to take pictures of the tested area with a standard camera and a thermal camera, with the aim of evaluating the evolution of the damage pattern. The final permanent deformation was measured with a caliper at the end of APT session 2 in order to evaluate the rutting performance of each test section.

The second part of the testing program focused on the laboratory characterization of slabs taken from the four test fields. Prismatic specimens ($30.5 \times 8.5 \times 8$ cm^3) obtained from the slabs were subjected to three point bending tests, carried out at 20 °C and a constant rate of 50.8 mm/min considering three repetitions, in order to assess the cracking resistance to flexural loads. It should be pointed out that the slabs were taken from the pavement area where APT was performed (specifically, from FC section). For R1 and R2, the laboratory results for field specimens (IN-SITU) were also compared with the corresponding results for laboratory-compacted slabs (LAB) with the same geocomposites at the interface and target air void content of 5 %, studied in a previous experimental investigation [14].

3. Results and analyses

3.1. Permanent deformation behaviour from APT

Despite APT was performed on a thin asphalt pavement, no cracks were observed in any test field (neither in the FC sections nor in the RC sections), as confirmed also by the images taken with camera and thermal camera. Instead, a remarkable permanent deformation beneath the load plate occurred in all cases.

In order to provide a possible explanation of this finding, the *equivalent single axle loads* (*ESALs*) corresponding to the loads applied (Table 1) were calculated (Eq. (1)).

$$ESALs = \sum_{i=1}^{n} LEF_i \cdot N_i \tag{1}$$

where N_i is the number of load applications of the generic "*i*" single axle and LEF_i is the load equivalency factor corresponding to the "*i*" single axle. LEF_i is defined as the ratio between the number of load applications of the reference single axle (N_{ref}) and the number of load applications of the generic single axle (N_i) that cause the same damage to the pavement and can be expressed as in Eq. (2), according to [16] and following studies.

$$LEF_i = k_a \cdot k_t \cdot k_p \cdot (P_i / P_{ref})^{\gamma} \tag{2}$$

where k_a, k_t and k_p are coefficients that take into account the effect of axle type, tire type and tire inflation pressure, respectively; P_i and P_{ref} indicate the load on the "*i*" single axle and on the reference single axle, respectively; γ is the exponent that governs the *LEF* law. The first study to develop the *LEF* law was the AASHO Road Test in the early 60 s [17] and, based on the outcomes of such experiment, the exponent γ is commonly assumed equal to 4. Subsequent studies [18–23], however, have shown that the value of γ may vary depending on the type of distress considered. Specifically, γ = 4 seems to be reasonable in the case of rutting, whereas a value of γ between 1.5 and 2 appears to be more appropriate in the case of fatigue cracking.

For the case of interest, a different *LEF* was determined for every load P_i applied, corresponding to a different fall height (see Table 1), i.e. *i* = H1, H2, H3, H4. As for P_{ref}, a 12-ton single axle with twin wheels was considered as reference axle. γ was chosen equal to 2 for fatigue and equal to 4 for rutting, resulting in eight *LEF* to be determined overall, depending on the fall height and the distress type. Conversely, the coefficients k_a, k_t and k_p depended only on the FastFWD characteristics and were the same regardless of fall height and distress type (k_a = 2.91, k_t = 1.00, k_p = 1.30). Finally, the number of FastFWD drops for H1, H2, H3 and H4, which were different in the case of FC and RC sections (see Table 1), were considered as N_i in Eq. (1).

From Table 2, which summarizes the number of *ESALs* calculated, it can be observed that, for both FC and RC sections, the *ESALs* related to rutting are more than double of the *ESALs* related to fatigue. This might explain why no cracks were observed after APT on the pavement, which instead exhibited noticeable permanent deflections.

Table 1
Summary of APT program.

Session	FC section				RC section			
	N. of drops	Fall height	Load [kN]	Load [kPa]	N. of drops	Fall height	Load [kN]	Load [kPa]
1*	13500	H2	50	750	6000	H2	50	750
	1000	H3	75	1050	500	H3	75	1050
2**	900	H1	35	500	600	H1	35	500
	2100	H4	120	1700	1400	H4	120	1700

* performed on 16–20 July 2018.
** performed on 2–3 August 2018.

Table 2
Number of *ESALs*.

Distress type	FC section	RC section
Fatigue	81660	44246
Rutting	181070	111678

The pavement surface deflection recorded at the end of APT sessions for all test fields is shown in Fig. 1a (FC sections) and Fig. 1b (RC sections). For a thorough interpretation of these outcomes, the subbase (E2) and subgrade (Es) moduli, determined through FastFWD tests and back-calculation analysis with ELMOD software preliminarily to APT, should also be taken into account (Table 3). For FC sections (Fig. 1a), the maximum permanent deflection is about 20 mm, higher than the limit of 13 mm (half inch) usually associated with the pavement crisis due to the accumulation of permanent deformations, likely because of the high number of *ESALs* related to rutting (Table 2). However, it can be observed that all reinforced systems exhibit an increased permanent deformation resistance with respect to the unreinforced system, even though the UN test field is characterized by higher subbase and subgrade moduli (Table 3). Moreover, the maximum deflection can be considered comparable for R1, R2 and R3. Permanent deflections greater than 13 mm can be observed also for RC sections (Fig. 1b). It should be noted that these results were obtained in RC sections by applying a number of load repetitions equal to about half of those considered for FC sections (see Tables 1 and 2), because of the pavement weakening due to the artificial cracks. For RC sections, R2 and R3 test fields exhibit a similar permanent deflection, which is about 5 mm lower than that shown by UN and R1 fields. Also in this case, however, it should be considered that the test fields reinforced with R1 and R2 are characterized by unbound layers with lower stiffness (Table 3).

Since the asphalt pavement was composed of a total thickness of only 8 cm, such high values of permanent deflection can be mainly attributed to a plastic yielding of the unbound layers. This consideration is confirmed by the values of bulk density measured (according to the sealed specimen procedure in EN 12697-6 [24]) on the asphalt samples taken after APT sessions outside and inside the loading area. Indeed, from Table 4 it can be observed that the variation of the bulk density due to APT is too small to determine the values of permanent deformation observed.

Overall, the results presented in Fig. 1 indicate that, despite lower moduli of the unbound layers in the reinforced test fields (see Table 3), the geocomposites were generally able to improve the permanent deformation resistance of the system. This finding can be explained by considering that geocomposites affect the spreading of vertical loads, leading to reduced and more even stress-strain distribution on the top of unbound layers.

Consequently, the vertical compression strain at the top of the subgrade for the reinforced system ($\varepsilon_z{}^R$) can be expressed as the corresponding strain for the unreinforced system ($\varepsilon_z{}^{UN}$) multiplied by a *mitigation coefficient* (α) lower than 1 (Eq. (3)).

$$\varepsilon_z^R = \alpha \cdot \varepsilon_z^{UN} \tag{3}$$

The mitigation coefficient can be estimated by considering the model developed by Ullidtz [25] based on the outcomes of APT carried out under conditions similar to this study (thin asphalt pavement 10 cm thick on a granular subbase course 15 cm thick). The model provides a correlation between the permanent deflection at the surface (*RD*, in mm) and the vertical compression strain at the top of the subgrade (ε_z), as in Eq. (4).

$$RD = 4.1\ \ mm \cdot MN^{0.333} \cdot (\varepsilon_z/1000\ \ \mu strain)^{1.333} \cdot (E/40\ \ MPa)^{0.333} \tag{4}$$

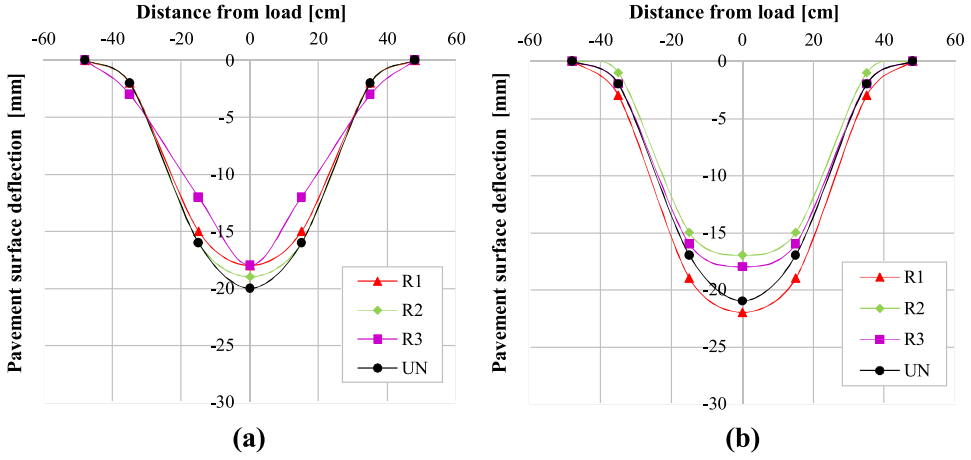

Fig. 1. Pavement surface deflection at the end of APT for (a) FC sections and (b) RC sections.

Table 3
Subbase (E2) and subgrade (Es) moduli.

Test field	E2 [MPa]	Es [MPa]
R1	89	49
R2	81	57
R3	133	72
UN	163	78

Table 4
Bulk density of the samples taken outside and inside the loading area.

Test field	Bulk density [g/cm^3]	
	Outside	Inside
R1	2.19	2.19
R2	2.15	2.21
R3	2.16	2.18
UN	2.16	2.20

where *MN* is the number of load applications (millions) and *E* is the subgrade modulus (MPa). In this study, the same number of load applications was adopted for all test fields and therefore, considering the ratio between the surface permanent deflection of the reinforced system (RD^R) and that of the unreinforced system (RD^{UN}), Eq. (5) can be derived.

$$\varepsilon_z^R = [(RD^R/RD^{UN})\cdot(E^{UN}/E^R)^{0.333}]^{(1/1.333)}\cdot\varepsilon_z^{UN} \tag{5}$$

where E^R and E^{UN} are the subgrade moduli for the reinforced and the unreinforced pavement, respectively. From the comparison between Eqs. (3) and (5), the expression of α can be easily deduced. It should be pointed out that Eq. (5) is based on the assumption that the model developed by Ullidtz [25] (shown in Eq. (4)) is valid also for reinforced pavements.

The values of the mitigation coefficient displayed in Fig. 2 are obtained, for each reinforced test field, as the average between α of the FC section and α of the RC section. Since the preliminary FastFWD tests were not carried out exactly in the same position as APT and considering also the slight inaccuracy of the back-calculation analysis, the values of α shown in Fig. 2 were determined by assuming the same subgrade modulus for the reinforced and the unreinforced systems (see Eq. (5)).

From Fig. 2, it can be observed that all the geocomposites studied are able to reduce the vertical compression strain at the top of the subgrade by about 5 % (R1) or 10 % (R2 and R3) as compared to the unreinforced system. This result indicates that, in terms of permanent deformation performance, the service life of thin asphalt pavements can be extended through the use of geocomposites.

3.2. Flexural behaviour from laboratory tests

The results of three point bending tests are usually expressed in terms of load-deflection (P–δ) curves (Fig. 3). The area below the curve until the flexural strength (P_{max}) represents the crack-initiation energy (E_i) (Fig. 3a), whereas the area below the curve from P_{max} to the specimen failure is the crack-propagation energy (E_p) (Fig. 3b). Specifically, for a double-layered specimen, the latter is given by the sum of the energy necessary for the propagation in the lower layer (E_{low}) and that necessary for the propagation in the upper layer (E_{up}). These contributions can be easily determined taking into account the specimen geometry. In previous studies [3], it has been observed that, in the case of reinforced pavements, the reinforcement mainly affects the crack propagation in the upper layer.

The results of the three point bending tests performed in a previous investigation on laboratory-compacted slabs [14] are shown in Fig. 4a. It can be observed that the unreinforced system (UN) exhibits a higher value of flexural strength (P_{max}) as compared to the reinforced systems (R1 and R2). This is ascribable to the de-bonding effect of the reinforcement at the interface [14]. However, after reaching P_{max}, UN rapidly loses its resistance until complete failure, without any residual flexural resistance. On the contrary, the reinforced systems show a significant post-peak dissipative phase (especially R2).

In order to quantify the contribution of the geocomposite in the crack-propagation phase, the *performance coefficient* (k), defined as in Eq. (6), was introduced.

$$k = E_{up}^R/E_{up}^{UN} \tag{6}$$

where $E_{up}{}^R$ and $E_{up}{}^{UN}$ represent the crack-propagation energy in the upper layer for the reinforced and the unreinforced system, respectively. It is worth pointing out that Eq. (6) is based on the assumption (supported by experimental observations) that the reinforcement does not influence the crack initiation and its propagation in the lower layer.

From the values of the performance coefficient shown in Fig. 4b (calculated for a maximum deflection of 15 mm), it can be observed that R1 and R2 increase the crack-propagation energy by about four times and nine times, respectively.

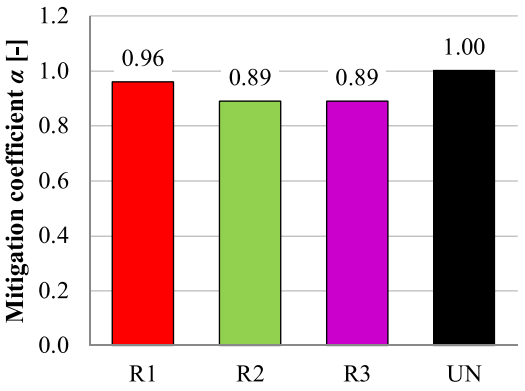

Fig. 2. Mitigation coefficient (α).

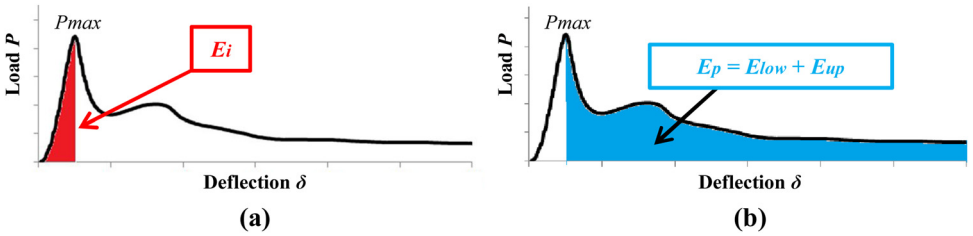

Fig. 3. (a) Crack-initiation energy (E_i), (b) crack-propagation energy (E_p).

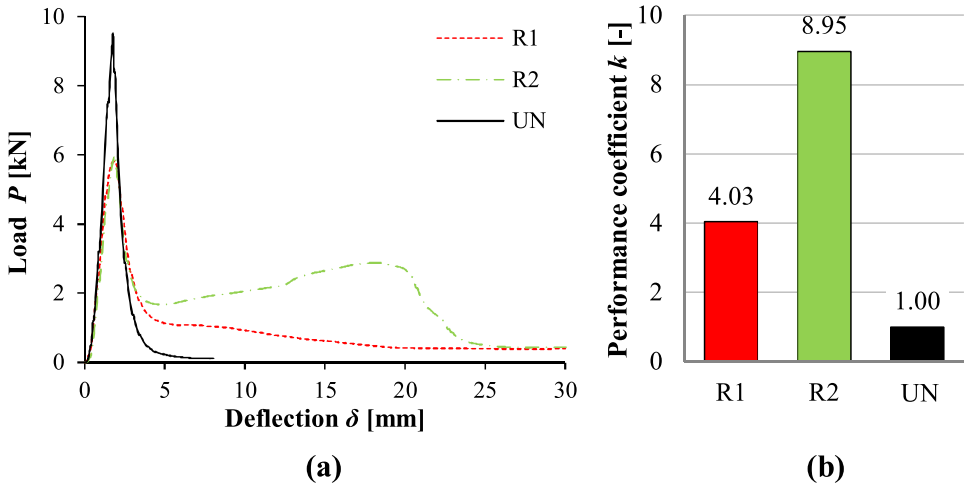

Fig. 4. Results of three point bending tests on laboratory-compacted specimens (LAB): (a) load-deflection curve, (b) performance coefficient.

Fig. 5a shows the load-deflection curves obtained for the specimens taken from the test fields of the trial section. As for the comparison between the different interfaces, observations similar to the case of LAB specimens (Fig. 4a) can be made. In addition, for the unreinforced pavement, P_{max} occurs at lower deflection with respect to the reinforced systems (Fig. 5a).

The values of k for IN-SITU specimens (calculated for a maximum deflection of 15 mm) are shown in Fig. 5b. Also in this case, it can be observed that all the geocomposites significantly increase the crack-propagation energy. Specifically, k is about 3 for R1, about 4.5 for R3 and about 8 for R2. Therefore, based on the experimental results, R2 is the reinforcement that delays the crack propagation the most.

These outcomes are confirmed also by the failure mechanisms observed on the specimens taken from the test fields, which are shown in Fig. 6. In fact, it can be noted that the presence of the geocomposite leads also to sub-horizontal crack propagation patterns parallel to the interface (especially for R2), whereas the crack propagation pattern is basically vertical for the unreinforced system (UN).

From the comparison between IN-SITU and LAB specimens (Figs. 4 and 5), it can be noted that the specimens prepared in the laboratory exhibit greater flexural strength (P_{max}) and slightly higher performance coefficient (k) with respect to the

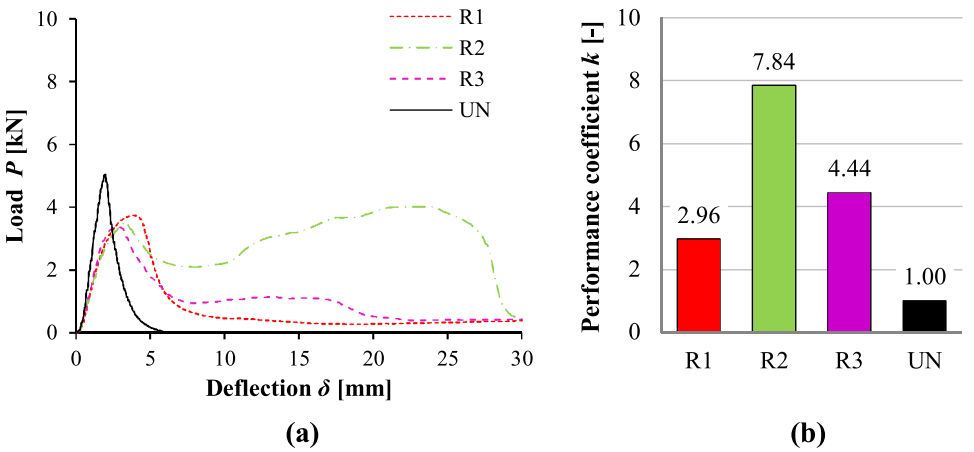

Fig. 5. Results of three point bending tests on specimens taken from the test fields (IN-SITU): (a) load-deflection curve, (b) performance coefficient.

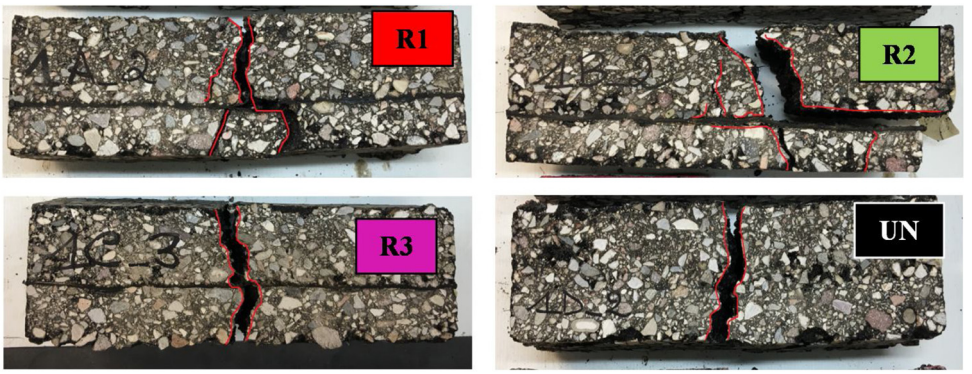

Fig. 6. Failure mechanism observed on three point bending specimens taken from the test fields (IN-SITU).

specimens taken from the trial section. Such differences may be due to the fact that the IN-SITU samples were taken exactly from the pavement area where APT was performed, and therefore they were already affected by a certain degree of damage. In addition, the IN-SITU shear resistance was lower than that observed on the LAB slabs [14], probably because of a non-perfect IN-SITU compaction and of the high melting temperature of the geocomposites' polypropylene upper surface (comparable to compaction temperatures, see Sections 2.1 and 2.2). A non-perfect IN-SITU compaction might have implied also a higher air void content for the IN-SITU specimens as compared to the LAB specimens. Another possible reason for the difference between IN-SITU and LAB specimens is that the materials used for the asphalt mixture (in terms of aggregates and bitumen) were very similar but not exactly the same. Nevertheless, it should be emphasized that the values of k are generally comparable in the two cases and the same ranking of the geocomposites (R1 and R2) is observed from the results of IN-SITU and LAB specimens, suggesting that the approach based on the evaluation of the k parameter can be considered reliable for assessing the performance of reinforced pavements.

Overall, these results indicate that, even though the reinforcement is not able to provide increased stiffness to the pavement structure [14], geocomposites can significantly extend the service life of thin asphalt pavements in terms of cracking by delaying the crack propagation in the upper layer.

4. Conclusions

This study focused on the effect of geocomposite reinforcement on the performance of thin asphalt pavements in terms of fatigue cracking, reflective cracking and permanent deformation accumulation. For this purpose, a full-scale trial section was constructed with four different types of interfaces: reinforced with geocomposites formed by the combination of a bituminous membrane with a fabric or grid (R1, R2, R3) and unreinforced (UN). The experimental program included APT carried out by means of FastFWD and laboratory tests (three point bending tests) performed on samples taken from the trial section. Moreover, the laboratory results (IN-SITU) were compared with those obtained in a previous investigation for laboratory-compacted slabs (LAB) with the same interface.

The main conclusions can be summarized as follows:

- no cracks were observed in the test fields after APT, whereas a significant permanent deformation occurred in all cases, probably because the *ESALs* related to rutting were more than double of the *ESALs* related to fatigue;
- the high permanent deflections emerged were likely caused by the plastic yielding of the unbound layers, as suggested by the similar values of the asphalt bulk density outside and inside the loading area;
- all the geocomposites improved the permanent deformation resistance of the pavement by reducing the vertical compression strain at the top of the subgrade. This reduction was about 5 % for R1 and 10 % for R2 and R3 as compared to the unreinforced pavement;
- the geocomposites increased the energy necessary for the crack propagation by three times (R1) to eight times (R2) as compared to the unreinforced pavement (R3 showed intermediate performance);
- the specimens prepared in the laboratory exhibited a better flexural behaviour with respect to the specimens taken from the trial section. This difference was probably due to the fact that the IN-SITU specimens were already characterized by a certain degree of damage and presented lower compaction degree and reduced shear resistance. Nevertheless, in the crack-propagation phase, such difference was relatively small and the same ranking of the geocomposites was observed from testing IN-SITU and LAB specimens;
- as for the comparison between the geocomposites, R2 showed the best performance in terms of permanent deformation resistance and flexural behaviour, followed by R3 and R1.

Overall, these findings indicate that geocomposites can extend the service life of thin asphalt pavements in terms of both permanent deformation accumulation and cracking.

Declaration of Competing Interest

The authors declare that they have no known competing financial interests or personal relationships that could have appeared to influence the work reported in this paper.

Acknowledgements

The activities presented in this paper were sponsored by Copernit S.p.A. (Italy), which gave both financial and technical support for the research project. The results and opinions presented are those of the authors.

References

[1] R.A. Austin, A.J.T. Gilchrist, Enhanced performance of asphalt pavements using geocomposites, Geotext Geomembr. 14 (3–4) (1996) 175–186.
[2] S.F. Brown, N.H. Thom, P.J. Sanders, A study of grid reinforced asphalt to combat reflection cracking, J. Assoc. Asphalt Paving Technol. 70 (2001) 543–569.
[3] F. Canestrari, L. Belogi, G. Ferrotti, A. Graziani, Shear and flexural characterization of grid-reinforced asphalt pavements and relation with field distress evolution, Mater. Struct. 48 (4) (2015) 959–975.
[4] G. Ferrotti, F. Canestrari, E. Pasquini, A. Virgili, Experimental evaluation of the influence of surface coating on fiberglass geogrid performance in asphalt pavements, Geotext Geomembr. 34 (2012) 11–18.
[5] F.M. Nejad, S. Asadi, S. Fallah, M. Vadood, Statistical-experimental study of geosynthetics performance on reflection cracking phenomenon, Geotext Geomembr. 44 (2016) 178–187.
[6] J.N. Prieto, J. Gallego, I. Perez, Application of the wheel reflective cracking test for assessing geosynthetics in anti-reflection pavement cracking systems, Geosynth Int. 14 (5) (2007) 287–297.
[7] S. Saride, V.V. Kumar, Influence of geosynthetic-interlayers on the performance of asphalt overlays on pre-cracked pavements, Geotext Geomembr. 45 (2017) 184–196.
[8] K. Sobhan, V. Tandon, Mitigating reflection cracking in asphalt overlay using geosynthetic reinforcements, Road Mater. Pavement Des. 9 (3) (2008) 367–387.
[9] E. Pasquini, M. Bocci, F. Canestrari, Laboratory characterisation of optimised geocomposites for asphalt pavement reinforcement, Geosynth Int. 21 (1) (2014) 24–36.
[10] G. Ferrotti, F. Canestrari, A. Virgili, A. Grilli, A strategic laboratory approach for the performance investigation of geogrids in flexible pavements, Constr. Build. Mater. 25 (2011) 2343–2348.
[11] E. Pasquini, M. Bocci, G. Ferrotti, F. Canestrari, Laboratory characterisation and field validation of geogrid-reinforced asphalt pavements, Road Mater. Pavement Des. 14 (2013) 17–35.
[12] D. Zamora-Barraza, M.A. Calzada-Pérez, D. Castro-Fresno, A. Vega-Zamanillo, New procedure for measuring adherence between a geosynthetic material and a bituminous mixture, Geotext Geomembr. 28 (5) (2010) 483–489.
[13] A. Saeed, J.W. Hall, NCHRP Report 512 – Accelerated Pavement Testing: Data Guidelines, Transportation Research Board, Washington DC, 2003.
[14] D. Ragni, T. Montillo, A. Marradi, F. Canestrari, Fast falling weight accelerated pavement testing and laboratory analysis of asphalt pavements reinforced with geocomposites, Lect Notes Civil Eng. 48 (2020) 417–430.
[15] M. Manosalvas-Paredes, A. Navarro Comes, M. Francesconi, S. Khosravifar, P. Ullidtz, Fast falling weight deflectometer (FastFWD) for accelerated pavement testing (APT), in: A. Loizos, I. Al-Qadi, T. Scarpas (Eds.), Bearing Capacity of Roads, Railways and Airfields: Proceedings of the 10th International Conference on the Bearing Capacity of Roads, Railways and Airfields (BCRRA 2017), June 28–30, 2017, CRC Press (Taylor & Francis Group), Athens, Greece, 2018, pp. 2235–2241.
[16] Organization for economic Co-operation and development, Road research group Paris, Impact of Heavy Freight Vehicles, (1983) .
[17] AASHTO, The AASHO Road Test: Report 7 – Summary Report, Highway Research Board Special Report 61G, Publication N. 1061, Highway Research Board, Washington DC, 1962.
[18] G. Battiato, G. Camomilla, M. Malgarini, C. Scapaticci, Measurements of the “Aggressiveness” of Goods Traffic on Road Pavement – Nardò Experiment, Report n. 3 – Tandem Effect Evaluation Autostrade 1, (1983) .

[19] S.H. Carpenter, Load equivalency factors and rutting rates: the AASHO Road Test, Transp. Res. Rec. 1354 (1992) 31–38.
[20] J.T. Christison, Pavement response to heavy truck axle loadings: the Canadian vehicle weights and dimensions study, Paper Presented at the International Symposium on Heavy Vehicle Weight and Dimensions, Kewlona, British Columbia, June 8–13, 1986, 1986.
[21] M. Huhtala, J. Pihlajamaki, M. Pienimaki, The effect of tire and tire pressure on road pavements, Transp. Res. Rec. 1227 (1989) 107–114.
[22] Organization for economic Co-operation and development, Road research group Paris, OECD Full Scale Pavement Test, (1991) .
[23] J.B. Rauhut, Development of pavement load equivalence factors using predictive damage models, Paper Presented at the FHWA Load Equivalence Workshop, McLean VA, 1988.
[24] EN 12697-6, Bituminous Mixtures - Test Methods for Hot Mix Asphalt - Part 6: Determination of Bulk Density of Bituminous Specimens, (2012) .
[25] P. Ullidtz, Simple model for pavement damage, Transp. Res. Rec. 1905 (2005) 128–137.